

## Heavy ion radiobiology

# Susceptible genes and molecular pathways related to heavy ion irradiation in oral squamous cell carcinoma cells

Kazuaki Fushimi<sup>a</sup>, Katsuhiko Uzawa<sup>a,\*</sup>, Takashi Ishigami<sup>a</sup>, Nobuharu Yamamoto<sup>f</sup>,  
Tetsuya Kawata<sup>b</sup>, Takahiko Shibahara<sup>f</sup>, Hisao Ito<sup>b</sup>, Jun-etsu Mizoe<sup>e</sup>,  
Hirohiko Tsujii<sup>e</sup>, Hideki Tanzawa<sup>a,c,d</sup>

<sup>a</sup>Department of Clinical Molecular Biology, and <sup>b</sup>Radiology, Graduate School of Medicine, Chiba University, <sup>c</sup>Division of Dentistry and Oral-Maxillofacial Surgery, Chiba University Hospital, <sup>d</sup>Center of Excellence (COE) Program in the 21st Century, Chiba University, <sup>e</sup>Research Center for Charged Particle Therapy, National Institute of Radiological Sciences, and <sup>f</sup>Department of Oral and Maxillo-Facial Surgery, Tokyo Dental College, Japan

## Abstract

**Background and purpose:** Heavy ion beams are high linear energy transfer (LET) radiation characterized by a higher relative biologic effectiveness than low LET radiation. The aim of the current study was to determine the difference of gene expression between heavy ion beams and X-rays in oral squamous cell carcinoma (OSCC)-derived cells.

**Materials and methods:** The OSCC cells were irradiated with accelerated carbon or neon ion irradiation or X-rays using three different doses. We sought to identify genes the expression of which is affected by carbon and neon ion irradiation using Affymetrix GeneChip analysis. The identified genes were analyzed using the Ingenuity Pathway Analysis Tool to investigate the functional network and gene ontology. Changes in mRNA expression in the genes were assessed by real-time quantitative reverse transcriptase-polymerase chain reaction (qRT-PCR).

**Results:** The microarray analysis identified 84 genes that were modulated by carbon and neon ion irradiation at all doses in OSCC cells. Among the genes, three genes (*TGFBR2*, *SMURF2*, and *BMP7*) and two genes (*CCND1* and *E2F3*), respectively, were found to be involved in the transforming growth factor  $\beta$ -signaling pathway and cell cycle:G1/S checkpoint regulation pathway. The qRT-PCR data from the five genes after heavy ion irradiation were consistent with the microarray data ( $P < 0.01$ ).

**Conclusion:** Our findings should serve as a basis for global characterization of radiation-regulated genes and pathways in heavy ion-irradiated OSCC.

© 2008 Elsevier Ireland Ltd. All rights reserved. Radiotherapy and Oncology 89 (2008) 237–244.

**Keywords:** Oral squamous cell carcinoma; Heavy ions; Microarray; Canonical pathway

The clinical management of oral squamous cell carcinoma (OSCC) causes oral sequelae that can compromise patient quality of life and necessitate abandonment or reduction of optimal therapeutic regimens, which in turn reduces the odds of long-term survival [10].

The use of a heavy ion beam for cancer therapy requires that some physical and biologic problems be solved. The narrow particle Bragg peak especially has to be widened so that it will cover the entire tumor volume. This broadening produces fluctuation of the linear energy transfer (LET) throughout the spread-out Bragg peak (SOBP). Any variation in LET also induces fluctuation of the relative biologic effectiveness (RBE). High LET heavy ion radiation is more effective than low LET X-rays for inducing biologic damage, it is generally characterized by an energy deposition peak at the end of its range, which provides good dose localization in critical cancer tissues and provides increased RBE in cell

killing within the peak. Tolerable damage to normal tissues and a destructive strike to cancerous cells, therefore, are expected with the use of heavy ion beam in cancer treatment.

Carbon ion beams emit high LET radiation characterized by higher RBE than low LET radiation, such as X-rays. Carbon ions were selected for clinical trials because they have the biologic characteristics of high LET with 78 keV/ $\mu$ m at the distal end of the SOBP and because they show good dose-localizing properties compared with heavier ions. These advantages have been shown in various cancers including sarcoma, melanoma, adenoid cystic carcinoma, adenocarcinoma, chordoma, and squamous cell carcinoma [1,16,22,23,26,27,29,33].

In previous studies, we successfully used microarray analysis to identify and classify a set of human genes that are characteristic of X-ray or carbon ion-irradiated OSCC cells.

We have shown that elevated levels of numerous genes (*Cytokeratin 18*, *DTNBP1*, *ASNA1*, *Tcp20*, *Cyclophilin F*, *KIAA0218*, *HBp17*, *PEG10*, *ROBO1*, *ICAM2*, *TIMP3*, *DAB2*, *MMP13*, *PLAGL1*, *ID1*, *PVRL3*, *ID3*, and *FGFR3*) may be associated with increased radioresistance [13,15] and that gene expression of *SPHK1* was altered by carbon irradiation in a dose- and time-dependent manner [12]. This purpose of analyzing the gene changes following the two types of heavy particle irradiation (carbon and neon ion) was to identify the genes with more heavy particle features.

In the current study, we performed microarray analysis using high-density Affymetrix U133A GeneChip arrays (Affymetrix, Santa Clara, CA) to assess the gene expression changes in OSCC cells after carbon and neon ion irradiation. Further, the genes identified were analyzed for network and gene ontology by Ingenuity Pathway Analysis (IPA) software (Ingenuity Systems, Mountain View, CA) to identify networks of interacting genes, other functional groups, and corresponding canonical pathways [17]. In addition, other selected genes confirmed the microarray data by real-time quantitative reverse transcriptase-polymerase chain reaction (qRT-PCR). The aim of the current study was to determine the difference of gene expression between heavy ion beams and X-rays in oral squamous cell carcinoma (OSCC)-derived cells.

## Materials and methods

### Cell line and culture conditions

The human OSCC-derived cell line Ca9-22 cells (Human Science Research Resources Bank, Osaka, Japan) were prepared for this study. The cells were maintained in Dulbecco's modified Eagle's medium F-12 HAM (Sigma Chemical Co., St. Louis, MO) and supplemented with 10% heat-inactivated fetal bovine serum and 50 U/ml penicillin and streptomycin. All cultures were grown at 37 °C in a humidified atmosphere of 5% carbon dioxide for routine growth.

### Irradiation using heavy ion beams and X-rays

All procedures of carbon and neon ion irradiation were carried out at the National Institute of Radiologic Sciences. Briefly, 290- and 400-MeV/nucleon carbon and neon ion beams, with 6-cm SOBP, were used through the experimental ports, and the RBE was set to 2.5 and 3.0 for carbon and neon, respectively. Cells plated in 75 cm<sup>2</sup> plastic flasks (Corning Inc., Corning, NY) were irradiated at the distal end of the SOBP (LET = 75,188 keV/μm). Three irradiated dose points (1, 4, and 7 Gy) were set.

In addition, the cells grown in 10-cm tissue culture dishes were irradiated with one dose of radiation (2, 4, and 8 Gy) using X-ray irradiation equipment (MBR-1520R-3; Hitachi, Tokyo, Japan) at Chiba University at a source-to-target distance of 55 cm when the cells were 70–80% confluent.

### Isolation of RNA

Total RNA was extracted with Trizol reagent (Invitrogen Life Technologies, Carlsbad, CA) from irradiated and unirradiated cells 4 h after irradiation, according to the manufac-

turer's instructions. The quality of total RNA was determined by Bioanalyzer (Agilent Technologies, Palo Alto, CA).

### Hybridization of RNAs to oligonucleotide arrays and data analysis

For microarray analysis, 4 h after irradiation was selected as the time point at which to monitor the early response of Ca9-22 cells to carbon or neon ions or X-ray irradiation and to identify differentially expressed early genes that mediate cellular events such as DNA repair and apoptosis. We used Human Genome U133A Array GeneChip oligonucleotide arrays. This GeneChip, containing 22,283 probe sets, analyzes the expression level of over 18,400 transcripts and variants, including 14,500 well-characterized human genes. One sample for each irradiated and unirradiated group was analyzed and the RNA following X-ray and carbon irradiation was the same RNA as used previously [12]. For hybridization, 20 μg of total RNA per sample was prepared according to the manufacturer's protocols (Affymetrix). Fragmented cRNA (15 μg of each) was hybridized to the Human Genome oligonucleotide arrays. The arrays were stained with phycoerythrin–streptavidin and the signal intensity was amplified by treatment with a biotin-conjugated antistreptavidin antibody, followed by a second staining using phycoerythrin–streptavidin. The arrays stained a second time were scanned using the Affymetrix GeneChip Scanner 3000.

GeneChip analysis was performed based on the Affymetrix GeneChip Manual (Affymetrix Inc.) with Microarray Analysis Suite 5.0, Data Mining Tool 2.0, and Microarray Database software. All genes on the GeneChip were globally normalized and scaled to a signal intensity of 500. The Microarray Analysis Suite software used Wilcoxon's test to generate detected (present or absent) calls and used the calls to statistically determine if a transcript was expressed or not. After being filtered through a "present" call ( $P < 0.05$ ), the expression data were analyzed using GeneChip Operating Software 1.1 (Affymetrix) and GeneSpring 6.1 (Silicon Genetics, Redwood City, CA). Fold changes were calculated by comparing transcripts between irradiated Ca9-22 cells and unirradiated Ca9-22 cells. We identified 84 genes differentially expressed by 2.0-fold or more by heavy ion irradiation at all doses (1, 4, and 7 Gy) and not substantially altered by X-rays.

### Genetic network analysis and canonical pathway analysis

The genes, which were identified by microarray analyses, were used for network and gene ontology analyses. Gene accession numbers were imported into the IPA software. Using the software, the genes were categorized based on location, cellular components, and reported or suggested biochemical, biologic, and molecular functions. The identified genes were also mapped to genetic networks available in the Ingenuity database and then ranked by score, which is the probability that a collection of genes equal to or greater than the number in a network could be achieved by chance alone. A score of 3 indicated a 1/1000 chance that the focus genes were in a network due to random chance. Therefore, scores of 3 or higher had a 99.9% confidence level of not

being generated by random chance alone. This score was used as the cut-off for identifying gene networks. Moreover, relationships between the network generated in IPA and the known pathways that were associated with metabolism and signaling were investigated by canonical pathway analysis.

### Preparation of cDNA

Total RNA was extracted using TRIzol reagent from carbon and neon ions and X-ray irradiated and unirradiated Ca9-22 cells. Total RNA samples were extracted 4 h after 1, 4, and 7 Gy of carbon and neon ions, and 2, 4, and 8 Gy X-ray irradiation to determine the dose-dependent effects,

according to the manufacturer's instructions. Five micrograms of total RNA of each sample was reversed transcribed to cDNA using Ready-to-Go You-Prime first-strand beads (GE Healthcare, Little Chalfort, Buckinghamshire, UK) and oligo(dT) primer (Sigma Genosys, Ishikari, Japan), according to the manufacturer's protocol.

### Analysis of mRNA expression by qRT-PCR

Real-time qRT-PCR was performed to verify the microarray data with a single method using a LightCycler Fast-Start DNA Master SYBR Green I kit (Roche Diagnostics GmbH, Mannheim, Germany), according to the procedure

Table 1  
Primers used for qRT-PCR

Gene name	Forward primer	Reverse primer	Size (bp)
<i>TGFBR2</i>	5'-TGCTGTGGATGACCTGGCTAA-3'	5'-TTCTAGGACTTCTGGAGCCATGT-3'	71
<i>BMP7</i>	5'-GCCAACGTGGCAGAGAACA-3'	5'-TGACATACAGCTC GTGCTTCTTACA-3'	67
<i>SMURF2</i>	5'-ACCATATAACAAGAACTACGCAATGG-3'	5'-TAAGAGGTCTGCCAGGGCTAGA-3'	78
<i>CCND1</i>	5'-GCATGTTCTGTGGCCTCTAAGA-3'	5'-CGGTGTAGATGCACAGCTTCTC-3'	69
<i>E2F3</i>	5'-ACTCCAAATCTCCCTCAGAAAAA-3'	5'-CAGGAGCTGAATGAACCTCTTGGT-3'	78
<i>GAPDH</i>	5'-CATCTCTGCCCTCTGCTGA-3'	5'-GGATGACCTTGCCACAGCCT-3'	305

bp, base pair.

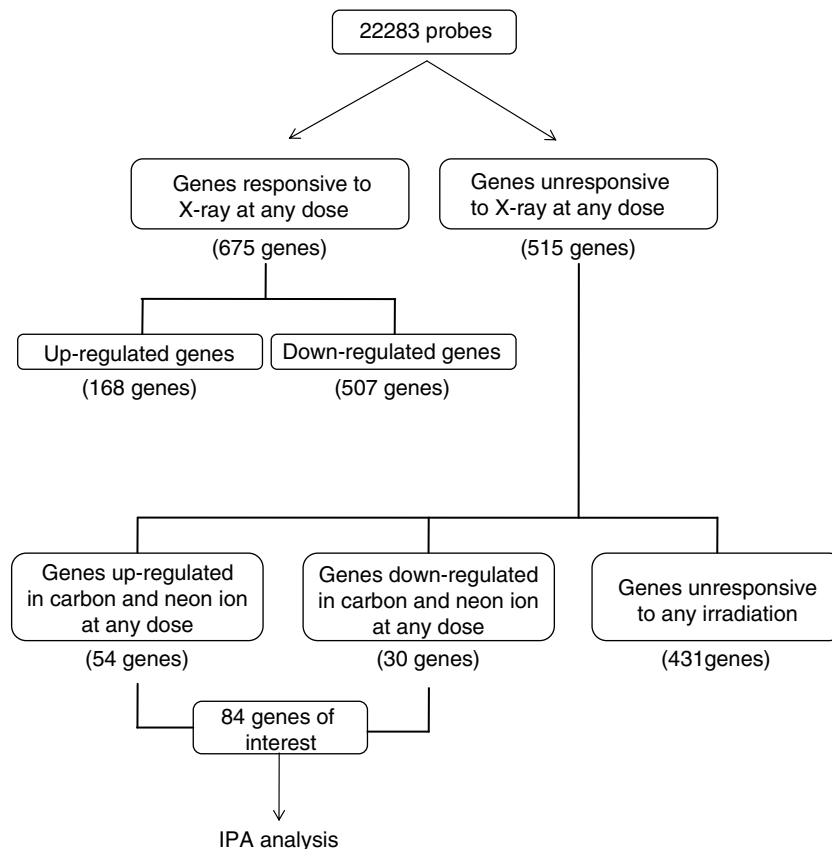


Fig. 1. Flowchart of gene analyzed after heavy ion irradiation and X-ray irradiation. The gene expression levels were compared directly with the fold-changes of the irradiated and unirradiated cells. Among the 22,283 probes tested with X-ray irradiation in Ca9-22 cells, we found that 675 genes (168 up-regulated and 507 down-regulated) changed, while 515 genes were unchanged at any dose. Among the unchanged genes, 431 genes were identified as unresponsive genes to any type of irradiation tested (carbon ion, neon ion, and X-ray), and they were excluded from further analysis. The remaining 84 genes with changes more than double or less than double were analyzed further by the IPA analysis.

Table 2 Genetic networks in the heavy ion-irradiated OSCC cells			
Network	Gene	Function	Score <sup>a</sup>
1	<u>ADCY7</u> , <u>ANXA1</u> , <u>AXL</u> , <u>CA2</u> , <u>CCND1</u> , <u>CD55</u> , <u>CD59</u> , <u>CEBPA</u> , <u>CEL</u> , <u>CETP</u> , <u>COL1A1</u> , <u>DDX21</u> , <u>DUSP1</u> , <u>E2F3</u> , <u>EPHX1</u> , <u>ESR1</u> , <u>FYN</u> , <u>GRB2</u> , <u>HBP1</u> , <u>ID2</u> , <u>IFI27</u> (includes EG:3429), <u>KLF9</u> , <u>MAL</u> , <u>MALT1</u> , <u>MYOD1</u> , <u>NP</u> , <u>NROB2</u> , <u>PAK6</u> , <u>PTPRE</u> , <u>S100G</u> , <u>SERPINF1</u> , <u>SOD2</u> , <u>TCF12</u> , <u>TGFA</u> , <u>TNFSF10</u>	Cancer, cell death, hematologic disease	30
2	<u>ACVRL1</u> , <u>ADRB2</u> , <u>AKAP12</u> , <u>ATP2B1</u> , <u>BMP7</u> , <u>CCNB2</u> , <u>COL1A1</u> , <u>ENG</u> , <u>HES1</u> , <u>ICAM3</u> , <u>ID2</u> , <u>ITGA2</u> , <u>ITGA5</u> , <u>ITGAD</u> , <u>ITGB1</u> , <u>KRT5</u> , <u>KRT8</u> , <u>KRT18</u> , <u>KRT19</u> , <u>MAML1</u> , <u>MAML2</u> , <u>MAML3</u> (includes EG:55534), <u>MYB</u> (includes EG:4602), <u>NOTCH3</u> , <u>PDE4D</u> , <u>PKP1</u> , <u>PODXL</u> , <u>PPAP2B</u> , <u>SPP1</u> , <u>TGFB2</u> , <u>TGFB3</u> , <u>TGFB2R</u> , <u>TP53</u> , <u>UPP1</u> , <u>VIL2</u>	Cellular movement, cardiovascular disease, cell cycle	23
3	<u>AR</u> , <u>CANX</u> , <u>CASP3</u> , <u>CDCP1</u> , <u>CFLAR</u> , <u>DKC1</u> , <u>EFNB2</u> , <u>EIF3S9</u> , <u>EIF3S10</u> , <u>ETV5</u> , <u>FOXO3A</u> (includes EG:2309), <u>GRIN1</u> , <u>HNRPC</u> , <u>IGF1</u> , <u>IGF2</u> , <u>IGFBP2</u> , <u>IL18</u> , <u>ISGF3G</u> , <u>LAMA3</u> , <u>M-RIP</u> , <u>MEN1</u> , <u>MYC</u> , <u>NEDD4L</u> , <u>PCBP2</u> , <u>PCBP1</u> (includes EG:5093), <u>PKN1</u> , <u>PLAT</u> , <u>PLD1</u> , <u>PLG</u> , <u>PMAIP1</u> , <u>SERPINC1</u> , <u>SMURF2</u> , <u>SPP1</u> , <u>TERT</u> , <u>YWHAZ</u>	Cancer, tumor morphology, cardiovascular disease	21
4	<u>ANK3</u> , <u>BCAT1</u> , <u>CCND3</u> , <u>CDKN2A</u> , <u>CLU</u> , <u>CSF2</u> , <u>DUSP1</u> , <u>ETS1</u> , <u>FOXO1</u> , <u>GSPT1</u> , <u>HIF1A</u> , <u>HMG2</u> , <u>HNRPA1</u> , <u>ID1</u> , <u>INSR</u> , <u>IPO7</u> , <u>KPNB1</u> , <u>LRCH4</u> , <u>MAPK8</u> , <u>MNT</u> , <u>MYC</u> <u>ODC1</u> , <u>PABPC1</u> , <u>PCBP1</u> (includes EG:5093), <u>PTHLH</u> , <u>PTPRC</u> , <u>RANBP1</u> , <u>RCC1</u> (includes EG:1104), <u>RPL10</u> , <u>SERPINB3</u> , <u>SNCG</u> , <u>SPP1</u> , <u>SYNCRIP</u> , <u>THY1</u> , <u>TIAM1</u>	Cell cycle, cancer, cell death	19

Underlining indicates genes identified by microarray analysis; other genes were either not on the expression array or did not change significantly.

<sup>a</sup> A score >3 is considered significant.

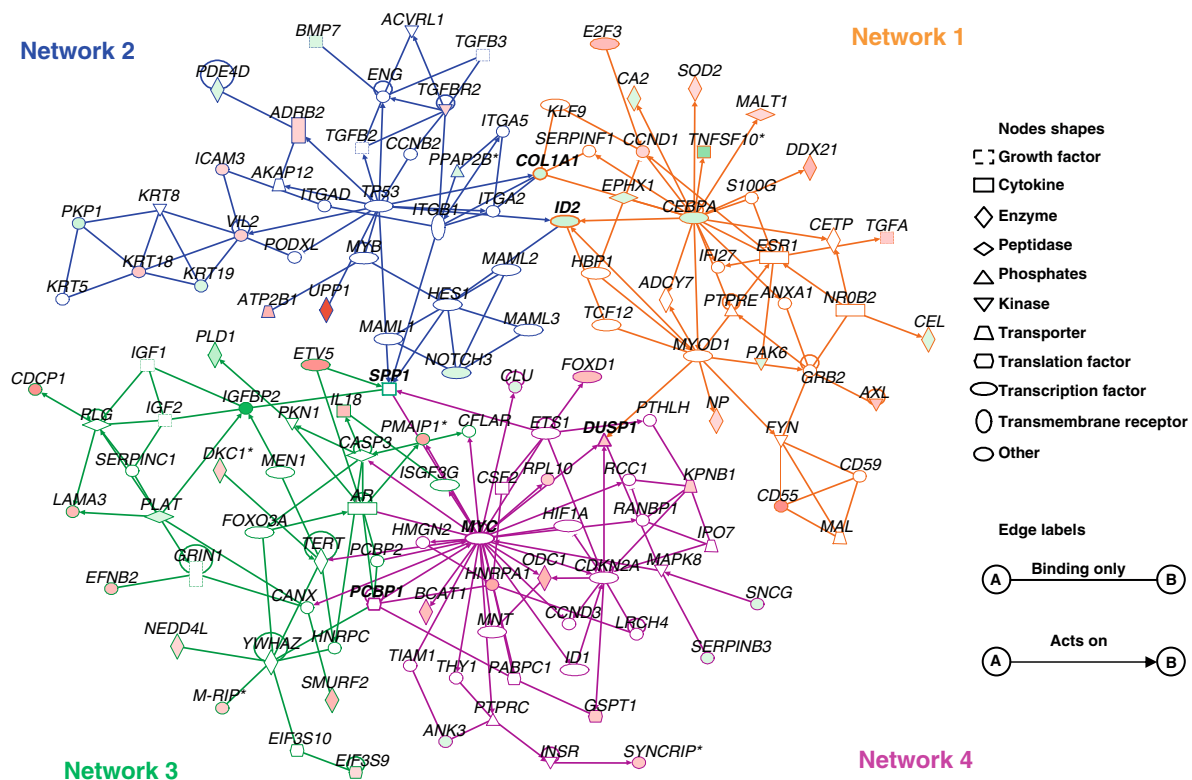


Fig. 2. Networks of genes modulated by heavy ion irradiation. IPA software was used to analyze the identified genes ( $n = 84$ ). Four networks were identified that were merged by overlapping genes (orange, network 1; blue, network 2; green, network 3; and purple, network 4). The intensity of node color indicates the degree of overexpression (red), and the degree of down-regulation (green) in heavy ion-irradiated Ca9-22 cells.

provided by the manufacturer. Oligonucleotides used as primers and the predicted sizes of amplified PCR products are listed in Table 1. Using LightCycler (Roche Diagnostics GmbH) apparatus, the experiment was carried out in a final

volume of 20  $\mu$ l of reaction mixture consisting of 2  $\mu$ l of FirstStart DNA Master SYBR Green I mix, 3 mM MgCl<sub>2</sub>, and 1  $\mu$ l of the primers according to the manufacturer's instructions. Subsequently, the reaction mixture was loaded into glass capillary tubes and subjected to an initial denaturation at 95 °C for 10 min, followed by 45 rounds of amplification at 95 °C (10 s) for denaturation, 62–64 °C (10 s) for annealing, and 72 °C for extension, with a temperature slope of 20 °C/s, performed in the LightCycler. The transcript amount for the genes differentially expressed in the microarray analysis was estimated from the respective standard curves and normalized to the glyceraldehyde-3-phosphate dehydrogenase (GAPDH) transcript amount determined in corresponding samples.

### Statistical analysis

The Student's *t*-test was used to determine the statistical significance of the associations between the mRNA expression levels of the irradiated and unirradiated cells. The criterion for statistical significance was  $P < 0.01$ .

## Results

### cDNA microarray analysis

The gene expression profiles of Ca9-22 cells exposed to carbon and neon ion and X-ray irradiation were analyzed using the high-throughput gene chip. We sought to identify genes consistently expressed within carbon and neon and X-ray irradiated Ca9-22 cells and unirradiated Ca9-22 cells. A total of 54 genes were overexpressed at least twofold both in carbon and neon-irradiated Ca9-22 cells at all dose points, while 30 genes were down-regulated at least twofold both in carbon and neon-irradiated Ca9-22 cells at all dose points (Fig. 1). Therefore, the results of microarray analysis showed that the expression levels of 84 genes were altered significantly by carbon and neon ion irradiation at all dose points in Ca9-22 cells compared with control Ca9-22 cells that were unirradiated; the expression levels were not significantly altered by X-ray irradiation at all dose points in Ca9-22 cells when compared to the control Ca9-22 cells.

### Genetic network analysis and canonical pathway analysis

We then investigated whether the 84 genes interacted biologically. Genetic network analysis of these genes was performed using the IPA tool. Among the 84 genes, we discovered 60 genes that mapped to four genetic networks (Table 2), which had at least one gene in common and were merged for display (Fig. 2). These networks indicated functional relationships between gene products based on known interactions in the literature. The results of the IPA tool showed that four networks were highly significant and that some common biological functions; cancer, cell death, cell cycle, were found in the four networks (Table 2). Several pathways with a known relation to cancer were observed in the canonical pathway analysis (Table 3). Among these pathways, TGF- $\beta$  signaling was statistically significant ( $P = 2.02 \times 10^{-2}$ ). Canonical pathway analysis revealed that the cell cycle was secondly important; network analysis

also showed that the cell cycle was one of the crucial functions induced by heavy ion irradiation (Fig. 3). Table 4 summarizes the related five genes identified as up-regulated or down-regulated with the Affymetrix GeneChip.

### Validation of microarray data by real-time qRT-PCR analysis

To verify the expression of the genes identified in microarray experiments, real-time qRT-PCR was performed using the same RNA as that used in the microarray analysis. We analyzed dose-dependent changes in the mRNAs of five genes by real-time qRT-PCR. The results of the quantitative assessment of the five genes are shown in Fig. 4. Consistent with the results of microarray analysis, there was a significant elevation of the expression levels of the five genes in all carbon and neon-irradiated Ca9-22 cells compared with unirradiated Ca9-22 cells ( $P < 0.01$ ). The data are expressed as the mean  $\pm$  SD of two-independent experiments with samples in triplicate.

Table 3  
Canonical pathway of heavy ion-enhanced genes

Canonical pathway	P value
TGF- $\beta$ signaling	2.02e-2
Cell cycle:G1/S checkpoint regulation	8.00e-2
Phospholipid degradation	8.29e-2
p38 MAPK signaling	1.22e-1
Valine, leucine and isoleucine biosynthesis	1.27e-1
Complement and coagulation cascades	1.49e-1
Pyrimidine metabolism	1.67e-1
cAMP-mediated signaling	1.79e-1
Glycerophospholipid metabolism	1.79e-1
Pantothenate and CoA biosynthesis	1.84e-1
Glycerolipid metabolism	1.90e-1
G-protein coupled receptor signaling	1.96e-1
Integrin signaling	2.16e-1
Axonal guidance signaling	2.41e-1
Urea cycle and metabolism of amino groups	2.46e-1
Nicotinate and nicotinamide metabolism	2.46e-1
Aminosugars metabolism	2.60e-1
NF- $\kappa$ B signaling	2.87e-1
Notch signaling	3.02e-1
Nitrogen metabolism	3.02e-1
Bile acid biosynthesis	3.09e-1
Sphingolipid metabolism	3.42e-1
Leukocyte extravasation signaling	3.65e-1
Wnt/ $\beta$ -catenin signaling	3.79e-1
GM-CSF signaling	3.92e-1
Death receptor signaling	4.03e-1
Valine, leucine and isoleucine degradation	4.54e-1
Arginine and proline metabolism	4.70e-1
Arachidonic acid metabolism	4.75e-1
IGF-1 signaling	4.85e-1
Neuregulin signaling	4.90e-1
IL-6 signaling	4.90e-1
PTEN signaling	5.00e-1
Protein ubiquitination pathway	5.36e-1
Cardiac $\beta$ -adrenergic signaling	5.56e-1
Starch and sucrose metabolism	5.56e-1
Actin cytoskeleton signaling	5.96e-1
PI3K/AKT signaling	6.02e-1



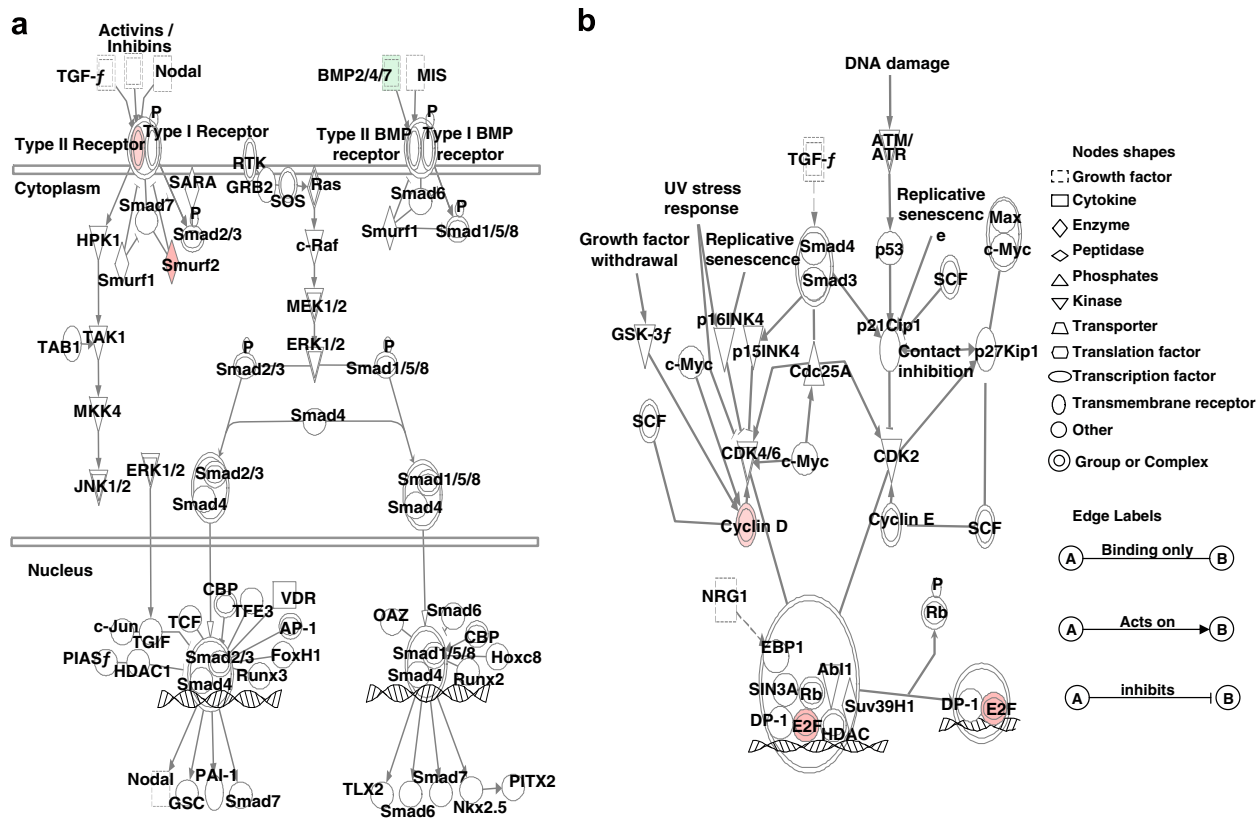


Fig. 3. IPA pathways integrating the expression data. The TGF- $\beta$  signaling pathway (a) and cell cycle/G1/S checkpoint regulation pathway (b) are significant in the whole data set. Red indicates up-regulated genes, and green indicates down-regulated genes. White indicates that the gene was not user specified but incorporated into the network through relationships.

Table 4 Irradiation-induced fold changes in the genes identified by canonical pathway analysis										
Gene symbol	Gene name	Fold changes								
		Carbon			Neon			X-ray		
		1 Gy	4 Gy	7 Gy	1 Gy	4 Gy	7 Gy	2 Gy	4 Gy	8 Gy
TGFBR2	Transforming growth factor, beta receptor II	2.61	2.38	2.30	2.41	2.59	2.50	1.26	1.43	1.11
SMURF2	E3 ubiquitin ligase	2.36	2.05	2.74	4.06	3.80	4.34	1.19	0.86	0.62
BMP7	Bone morphogenic protein 7	0.35	0.33	0.33	0.41	0.40	0.35	0.78	0.94	0.87
CCND1	Cyclin D1	2.66	3.86	3.66	5.60	4.26	4.35	1.29	1.20	1.11
F2F3	E2F transcription factor 3	2.67	2.81	2.71	2.60	4.66	4.31	1.13	0.92	0.61

The fold changes in the five genes after heavy ions and X-ray irradiation cells compared with unirradiated cells.

Moreover, the expression levels after X-ray irradiation were compared with the levels obtained before irradiation (0 Gy). The expression levels of the five genes changed little after X-ray irradiation in a dose-dependent manner, which validated the microarray data.

Discussion

High LET radiation, such as heavy ions, is more effective than low LET radiation for causing many kinds of biologic effects. Therefore, high LET radiation is more beneficial for treating malignant tumors than low LET radiation due to

the excellent dose localization and high relative biologic effectiveness. Recently, several studies have successfully used microarrays to identify and classify a set of human genes in response to ionizing radiation [7,8,11,18]. To date, no report has focused on the gene expression profiles of OSCC cells exposed simultaneously to X-ray and carbon and neon ion beam irradiation. To highlight the gene expression changes in OSCC cells exposed to carbon and neon ion beams, we used the high-throughput gene chip that contains 22,283 oligonucleotide-based probe sets to analyze dose-dependent gene expression changes after carbon and neon ion irradiation.

In the current study, we identified 84 genes that were modulated by carbon and neon ion irradiation at all doses in Ca9-22 cells using microarray analysis. We then analyzed these genes with regard to functional network and gene ontology using the IPA tool and detected four genetic networks, each of which was characterized by different representative functions. We found that networks 2 and 4 were significantly associated with the cell cycle. These networks are merged via overlapping genes (Fig. 2). In addition, two canonical pathways (TGF- $\beta$  signaling, cell cycle:G1/S checkpoint regulation) were significantly affected. TGF- $\beta$  is a potent growth inhibitor of most cell types; therefore, perturbations of TGF-signaling are believed to result in progression of various tumors [3]. However, TGF- $\beta$  acts as an oncogenic cytokine through induction of extracellular matrices, angiogenesis, and immunosuppression, indicating that TGF- $\beta$  facilitates tumor progression under certain conditions [5,34]. Two genes (*TGFBR2*, *SMURF2*) were up-regulated and one gene (*BMP7*) was down-regulated in this pathway. A recent time course study has shown expression of genes in ovarian cancer; genes that inhibit TGF- $\beta$  signaling (*DACH1*, *BMP7*, and *EVI1*) were up-regulated in advanced-stage ovarian cancers and, conversely, genes that enhance TGF- $\beta$  signaling (*PCAF*, *TFE3*, *TGFBR2*, and *SMAD4*) were down-regulated compared with normal samples [32]. Therefore, we suspect that overexpression of *TGFBR2* and underexpression of *BMP7* are key events in OSCC cells exposed to carbon and neon ion irradiation; because TGF- $\beta$  is a potent growth inhibitor of most cell types, perturbations of TGF- $\beta$  signaling result in progression of various tumors. *SMURF2* has been reported to be expressed in patients with esophageal squamous carcinoma [6], and high expression is correlated with poor prognosis of esophageal cancer.

It has been known for over 50 years that exposure of cells to IR delays the normal progression through the cell cycle [2,4,14,21]. Compared to cells in the G0G1 or G2M phase, cells in the S phase are radioresistance. This radioresistant can be overcome more readily by heavy ions than X-rays. The two genes associated with cell cycle:G1/S checkpoint regulation were *CCND1* and *E2F3*.

Excessive overexpression of *CCND1* that results from transient transfection may induce apoptosis on its own [9,19], whereas moderate overexpression of *CCND1*, as observed in stable transfectants, results in an accelerated transition through the G1 phase of the cell cycle in human fibroblasts [25,28] and leads to apoptosis only when cells are deprived of serum [30]. In mid- to late G1, hyperphosphorylation of pRb by the *CCND1/cdk4-cdk6* complex leads to release of *E2F1–3*, which binds to specific E2F-responsive promoters, stimulating the transcription of genes involved in G1/S progression [24,31]. Most cancer cells contain mutations that deregulate the pRb/E2F pathway, which highlights its relevance in the control of cellular proliferation. Deregulation of pRb/E2F pathway control can also result in activation of E2F1-induced apoptosis in several cell lines. *E2F3* has also been shown to stimulate apoptosis but in *E2F1*-dependent pathways [20]. Therefore, enhanced expression of *CCND1* and *E2F3* may affect regulation of the cell cycle and lead to apoptosis after heavy ion irradiation in OSCC.

In conclusion, global gene expression profiling and computational pathway analyses provide detailed knowledge of changes in gene expression induced by carbon and neon ion irradiation. We identified 84 genes that were characterized by carbon and neon ion irradiation. We further found that two canonical pathways (TGF- $\beta$  signaling, cell cycle: G1/S checkpoint regulation) had significant changes in gene expression. *TGFBR2*, *SMURF2*, *BMP7*, *CCND1*, and *E2F3* were

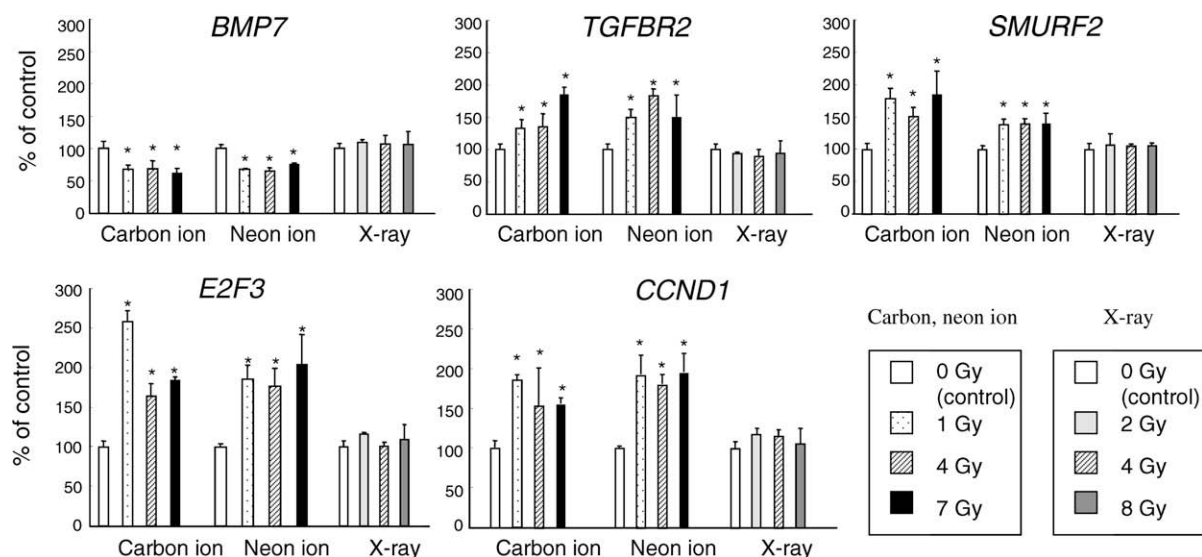


Fig. 4. Quantification of the mRNA levels of five genes 4 h after carbon and neon ion irradiation with 1, 4, and 7 Gy and after X-ray irradiation with 2, 4, and 8 Gy in Ca9-22 cells by qRT-PCR analysis. The results are normalized as a ratio of each specific mRNA signal to the *GAPDH* gene signal within the same RNA sample and then expressed as the percentage of the values obtained for control cells. Asterisks indicate significant differences in mRNA expression levels between control cells and carbon, neon-irradiated cells at each dose points ( $P < 0.01$ , Student's *t*-test). A significant elevation in the expression levels of the five genes in the carbon and neon-irradiated cells is confirmed by qRT-PCR analysis. In contrast, no or little change is evident in the expression levels of the five genes after X-ray irradiation. Data are expressed as mean  $\pm$  SD.

established as being centered in these genomic networks. Therefore, subsequent susceptibility of these five genes may occur specifically in the heavy ion-irradiated OSCC and is the difference in the response to the signal machinery of tumor morphology and cell cycle between the X-ray-irradiated cells and heavy ion-irradiated cells. There is an urgent need to examine the role of the genes in detail and to elucidate the regulatory mechanism of gene expression in OSCC cells exposed to heavy ion beams and X-ray irradiation.

#### Acknowledgement

We thank Lynda C. Charters for editing this manuscript.

\* **Corresponding author.** Katsuhiko Uzawa, Department of Clinical Molecular Biology, Graduate School of Medicine, Chiba University, 1-8-1 Inohana, Chuo-ku, Chiba 260-8670, Japan.

E-mail address: [uzawak@faculty.chiba-u.jp](mailto:uzawak@faculty.chiba-u.jp)

Received 3 July 2007; received in revised form 15 April 2008; accepted 25 April 2008; Available online 29 May 2008

#### References

- [1] Asakawa I, Yoshimura H, Takahashi A, et al. Radiation-induced growth inhibition in transplanted human tongue carcinomas with different p53 gene status. *Anticancer Res* 2002;22:2037–43.
- [2] Bernhard EJ, Maity A, Muschel RJ, McKenna WG. Effects of ionizing radiation on cell cycle progression. *Radiat Environ Biophys* 1995;34:79–83.
- [3] Blobel GC, Schiemann WP, Lodish HF. Role of transforming growth factor  $\beta$  in human disease. *N Engl J Med* 2000;342:1350–8.
- [4] Cann KL, Hicks GG. Absence of an immediate G1/S checkpoint in primary MEFs following gamma-irradiation identifies a novel checkpoint switch. *Cell Cycle* 2006;5:1823–30.
- [5] Derynck R, Akhurst RJ, Balmain A. TGF- $\beta$  signaling in tumor suppression and cancer progression. *Nat Genet* 2001;29:117–29.
- [6] Fukuchi M, Fukai Y, Masuda N, et al. High-level expression of the Smad ubiquitin ligase Smurf2 correlates with poor prognosis in patients with esophageal squamous cell carcinoma. *Cancer Res* 2002;62:7162–5.
- [7] Fukuda K, Sakakura C, Miyagawa K, et al. Differential gene expression profiles of radioresistant oesophageal cancer cell lines established by continuous fractionated irradiation. *Br J Cancer* 2004;91:1543–50.
- [8] Guo WF, Lin RX, Huang J, et al. Identification of differentially expressed genes contributing to radioresistance in lung cancer cells using microarray analysis. *Radiat Res* 2005;164:27–35.
- [9] Han EK, Begemann M, Sgambato A, et al. Increased expression of cyclin D1 in a murine mammary epithelial cell line induces p27kip1, inhibits growth, and enhances apoptosis. *Cell Growth Differ* 1996;7:699–710.
- [10] Hancock PJ, Epstein JB, Sadler GR. Oral and dental management related to radiation therapy for head and neck cancer. *J Can Dent Assoc* 2003;69:585–90.
- [11] Hellman B, Brodin D, Andersson M, et al. Radiation-induced DNA-damage and gene expression profiles in human lung cancer cells with different radiosensitivity. *Exp Oncol* 2005;27:102–7.
- [12] Higo M, Uzawa K, Kawata T, et al. Enhancement of SPHK1 in vitro by carbon ion irradiation in oral squamous cell carcinoma. *Int J Radiat Oncol Biol Phys* 2006;65:867–75.
- [13] Higo M, Uzawa K, Kouzu Y, et al. Identification of candidate radioresistant genes in human squamous cell carcinoma cells through gene expression analysis using DNA microarrays. *Oncol Rep* 2005;14:1293–8.
- [14] Iliakis G. Cell cycle regulation in irradiated and unirradiated cells. *Semin Oncol* 1997;24:602–15.
- [15] Ishigami T, Uzawa K, Higo M, et al. Genes and molecular pathways related to radioresistance of oral squamous cell carcinoma cells. *Int J Cancer* 2007;120:2262–70.
- [16] Kamada T, Tsujii H, Tsuji H, et al. Efficacy and safety of carbon ion radiotherapy in bone and soft tissue sarcomas. *J Clin Oncol* 2002;20:4466–71.
- [17] Kim Y, Ton TV, DeAngelo AB, et al. Major carcinogenic pathways identified by gene expression analysis of peritoneal mesotheliomas following chemical treatment in F344 rats. *Toxicol Appl Pharmacol* 2006;214:144–51.
- [18] Kitahara O, Katagiri T, Tsunoda T, Harima Y, Nakamura Y. Classification of sensitivity or resistance of cervical cancers to ionizing radiation according to expression profiles of 62 genes selected by cDNA microarray analysis. *Neoplasia* 2002;4:295–303.
- [19] Kranenburg O, van der Eb AJ, Zantema A. Cyclin D1 is an essential mediator of apoptotic neuronal cell death. *EMBO J* 1996;15:46–54.
- [20] Lazzerini Denchi E, Helin K. E2F1 is crucial for E2F-dependent apoptosis. *EMBO Rep* 2005;6:661–8.
- [21] Maity A, McKenna WG, Muschel RJ. The molecular basis for cell cycle delays following ionizing radiation: a review. *Radiother Oncol* 1994;31:1–13.
- [22] Miyamoto T, Yamamoto N, Nishimura H, et al. Carbon ion radiotherapy for stage I non-small cell lung cancer. *Radiother Oncol* 2003;66:127–40.
- [23] Mizoe JE, Tsujii H, Kamada T, et al. Dose escalation study of carbon ion radiotherapy for locally advanced head-and-neck cancer. *Int J Radiat Oncol Biol Phys* 2004;60:358–64.
- [24] Muller H, Bracken AP, Vernell R, et al. E2Fs regulate the expression of genes involved in differentiation, development, proliferation, and apoptosis. *Genes Dev* 2001;15:267–85.
- [25] Musgrove EA, Lee CS, Buckley MF, Sutherland RL. Cyclin D1 induction in breast cancer cells shortens G1 and is sufficient for cells arrested in G1 to complete the cell cycle. *Proc Natl Acad Sci USA* 1994;91:8022–6.
- [26] Nakano T, Suzuki M, Abe A, et al. The phase I/II clinical study of carbon ion therapy for cancer of the uterine cervix. *Cancer J Sci Am* 1999;5:362–9.
- [27] Oohira G, Yamada S, Ochiai T, et al. Growth suppression of esophageal squamous cell carcinoma induced by heavy carbon-ion beams combined with p53 gene transfer. *Int J Oncol* 2004;25:563–9.
- [28] Resnitzky D, Gossen M, Bujard H, Reed SI. Acceleration of the G1/S phase transition by expression of cyclins D1 and E with an inducible system. *Mol Cell Biol* 1994;14:1669–79.
- [29] Schulz-Ertner D, Nikoghosyan A, Thilmann C, et al. Results of carbon ion radiotherapy in 152 patients. *Int J Radiat Oncol Biol Phys* 2004;58:631–40.
- [30] Sofer-Levi Y, Resnitzky D. Apoptosis induced by ectopic expression of cyclin D1 but not cyclin E. *Oncogene* 1996;13:2431–7.
- [31] Stevaux O, Dyson NJ. A revised picture of the E2F transcriptional network and RB function. *Curr Opin Cell Biol* 2002;14(6):684–91.
- [32] Sunde JS, Donniger H, Wu K, et al. Expression of genes that contribute to the inhibition of transforming growth factor- $\beta$  signaling in ovarian cancer. *Cancer Res* 2006;66:8404–12.
- [33] Tsuji H, Ishikawa H, Yanagi T, et al. Carbon-ion radiotherapy for locally advanced or unfavorably located choroidal melanoma: a phase I/II dose-escalation study. *Int J Radiat Oncol Biol Phys* 2007;67:857–62.
- [34] Wakefield LM, Roberts AB. TGF- $\beta$  signaling: positive and negative effects on tumorigenesis. *Curr Opin Genet Dev* 2002;12:22–9.